

Dealing with Collinearity in Large-Scale Linear System Identification Using Gaussian Regression

Wenqi Cao ^a, Gianluigi Pillonetto ^b,

^a*Department of Automation, Shanghai Jiao Tong University, Shanghai, China*

^b*Department of Information Engineering, University of Padova, Padova, Italy*

Abstract

Many problems arising in control require the determination of a mathematical model of the application. This has often to be performed starting from input-output data, leading to a task known as system identification in the engineering literature. One emerging topic in this field is estimation of networks consisting of several interconnected dynamic systems. We consider the linear setting assuming that system outputs are the result of many correlated inputs, hence making system identification severely ill-conditioned. This is a scenario often encountered when modeling complex systems composed by many sub-units with feedback and algebraic loops. We develop a strategy cast in a Bayesian regularization framework where any impulse response is seen as realization of a zero-mean Gaussian process. Any covariance is defined by the so called stable spline kernel which includes information on smooth exponential decay. We design a novel Markov chain Monte Carlo scheme able to reconstruct the impulse responses posterior by efficiently dealing with collinearity. Our scheme relies on a variation of the Gibbs sampling technique: beyond considering blocks forming a partition of the parameter space, some other (overlapping) blocks are also updated on the basis of the level of collinearity of the system inputs. Theoretical properties of the algorithm are studied obtaining its convergence rate. Numerical experiments are included using systems containing hundreds of impulse responses and highly correlated inputs.

Key words: linear system identification, kernel-based regularization, Gaussian regression, stable spline kernel, collinearity, large-scale systems.

1 Introduction

Large-scale dynamic systems arise in many scientific fields like engineering, biomedicine and neuroscience, examples being sensor networks, power grids and the brain [15, 18, 24, 34]. Modeling these complex physical systems, starting from input-output data, is a problem known as system identification in the literature [21, 39]. It is a key preliminary step for prediction and control purposes [21, 39]. Often, the systems under study can be seen as networks composed of a large set of interconnected sub-units. They can thus be described through many nodes which can communicate each other through modules driven by measurable inputs or noises [7, 8, 10, 22, 41, 43].

In this paper we assume that linear dynamics underly our large-scale dynamic system and focus on the identi-

fication of Multiple Inputs Single Output (MISO) stable models. The problem thus reduces to estimation of impulse responses. In addition, the system output measurements are assumed to be the result of many measurable and highly correlated inputs, possibly also low-pass with poor excitation of system dynamics. Such scenario is not unusual in dynamic networks since modules interconnections give rise to feedback and algebraic loops [3, 11, 13, 17, 35, 42]. This complicates considerably the identification process: low pass and almost collinear inputs lead to severe ill-conditioning [5, Chapter 3] [9], as described also in real applications like [20, 23, 33]. This makes especially difficult the use of the classical approach to system identification [21, 39], where different parametric structures have to be postulated. For instance, the introduction of rational transfer functions to describe each impulse response leads to high-dimensional nonconvex optimization problems. In addition, the system dimension (i.e. the discrete order of the polynomials defining the rational transfer functions) has typically to be estimated from data, e.g. using AIC or cross validation [1, 16]. This further complicates the problem due to the combinato-

* This paper was not presented at any IFAC meeting. Corresponding author W. Cao.

Email addresses: wenqicao@sjtu.edu.cn (Wenqi Cao), giapi@dei.unipd.it (Gianluigi Pillonetto).

rial nature of model order selection.

The problem of collinearity in linear regression has been discussed for several decades [5, 40, 44]. Two types of methods are mainly considered. One consists of eliminating some related regressors, the other of exploiting special regression methods like LASSO, ridge regression or partial least squares [40]. The main idea underlying these approaches is to eliminate or decrease the influence of correlated variables. This strategy can be useful when the goal is to obtain a model useful for predicting future data from inputs with statistics very similar to those in the training set.

This paper follows a different route based on Bayesian identification of dynamic systems via Gaussian regression [4, 6, 31, 36]. It exploits recent intersections between system identification and machine learning which involve Gaussian regression, see also [25, 45] for other lines which combine dynamic systems and deep networks. In particular, we couple the stable spline prior proposed in [28–30] with a Markov chain Monte Carlo (MCMC) strategy [12] suited to overcome collinearity. These two key ingredients (stable spline and MCMC) of our algorithm are now briefly introduced. The stable spline kernel is a nonparametric description of stable systems: it embeds BIBO stability, one of the most important concepts in control which ensures that bounded inputs always produce bounded outputs. It has shown some important advantages in comparison with classical parametric prediction error methods [21, 26, 31]. It models an impulse response as a zero-mean Gaussian process whose covariance includes information on smooth exponential decay and depends on two hyperparameters: a scale factor and a decay rate [2, 27, 32]. The main novelty in this paper is that the stable spline kernel is implemented using a Full Bayes approach (hyperparameters are also modeled as random variables) coupled with an MCMC strategy able to deal with collinearity. MCMC is a class of algorithms that builds a suitable Markov chain which converges to the desired target distribution. In our case, the distribution of interest is the joint posterior of hyperparameters and impulse responses. To deal with collinearity, we design a new formulation of a particular MCMC scheme known as Gibbs sampling [12] able to visit more frequently those parts of the parameter space mostly correlated. In particular, beyond considering blocks forming a partition of the parameter space, some other (overlapping) blocks are also updated on the basis of the level of inputs correlation. Theoretical properties of this algorithm are studied obtaining its convergence rate. Such analysis is then complemented with numerical experiments. This allows to quantify the advantages of the new identification procedure both under a theoretical and an empirical framework.

The structure of the paper is as follows. Section 2 reports the problem statement by introducing the measurement model and the prior model on the unknown

impulse responses. In Section 3, we describe the system identification procedure, discuss the issues regarding the selection of the overlapping blocks to be updated during the MCMC simulation and the impact of stable spline scale factors on the estimation performance. Convergence properties of our algorithm are illustrated in Section 4. Section 5 reports three numerical examples which highlight accuracy and efficiency of the identification procedure under collinearity. Conclusions then end the paper while Appendix reports the proof of the main convergence result here obtained.

2 Problem Formulation and Bayesian model

2.1 Measurements model

Consider a node in a dynamic network associated to a measurable and noisy output denoted by y . We assume that such output is the result of many inputs u_k which communicate with such node through some linear and stable dynamic systems. The transfer function of each module is assumed to be rational, hence the z -transform of any impulse response is the ratio of two polynomials. This is one of the most important descriptions of dynamic systems encountered in nature. Specifically, the measurements model is

$$y(i) = \sum_{k=1}^m F_k u_k(i) + e(i), \quad i = 1, \dots, n \quad (1)$$

where the F_k are stable rational transfer functions sharing a common denominator, $y(i)$ is the output measured at t_i , $u_k(i)$ is the known input entering the k -th channel at time t_i , $m \geq 2$ is the number of modules influencing the node. Finally, the random variables $e(i)$ form a white Gaussian noise of variance σ^2 . The problem is to estimate the m transfer functions from the input-output samples. The difficulty we want to face is that the number of unknown parameters, given by the coefficients of the polynomials entering the F_k , can be relatively large w.r.t. the data set size n and some of the u_k may be highly collinear. Thinking of the inputs as realizations of stochastic process, this means that the level of correlation among the u_k can be close to 1. Also, the model order, defined by the degrees of the polynomials in the F_k , can be unknown.

2.2 Convexification of the problem and Bayesian framework

An important convexification of the model (1) is obtained approximating each stable F_k by a FIR model of order p sufficiently large. This permits to rewrite (1) in matrix-vector form. In particular, if $G_k \in \mathbb{R}^{n \times p}$ are suitable Toeplitz matrices containing past input values, one

has

$$Y = \left(\sum_{k=1}^m G_k \theta_k \right) + E = G\theta + E \quad (2)$$

where the column vectors Y, θ_k and E contain, respectively, the n output measurements, the p impulse response coefficients defining the k -th impulse response and the n i.i.d. Gaussian noises. Finally, on the rhs $G = [G_1 \dots G_m]$ while θ is the column vector which contains all the impulse response coefficients contained in the θ_k .

A drawback of the formulation (2) is that, even if FIR models are easy to estimate through linear least squares, they may suffer of large variance. This problem is especially relevant in light of the assumed collinearities among the inputs: the regression matrix G turns out to be ill-conditioned, with a very large condition number, so that small output noises can produce large estimation errors. This problem is faced by the Bayesian linear system identification approach documented in [30, 31]: for known covariance, the θ_k are modeled as independent zero-mean Gaussian vectors with covariances proportional to the stable spline matrix $K \in \mathbb{R}^{p \times p}$. Such matrix encodes smooth exponential decay information on the coefficients of θ_k : the i, j -entry of K is

$$K(i, j) = \alpha^{\max(i, j)}. \quad (3)$$

where α regulates how fast the impulse response variance decays to zero. This parameter is assumed to be known in what follows to simplify the exposition.

Differently from [30], the covariances of the θ_k depend on scale factors λ_k which are seen as independent random variables. Hence, beyond the impulse responses conditional on the λ_k , also the stable spline covariances $\lambda_k K$ become stochastic objects. The λ_k follow an improper Jeffrey's distribution [19]. Such prior in practice includes only nonnegativity information and is defined by

$$p(\lambda_k) \sim \frac{1}{\lambda_k} \quad (4)$$

where here, and in what follows, $p(\cdot)$ denotes a probability density function. In its more general form, our model assumes that all the scale factors λ_k are mutually independent. But, later on, we will also see that constraining all of them to be the same can be crucial to deal with collinearity. The noise variance σ^2 is also a random variable (independent of λ_k) and follows the Jeffrey's prior. Finally, for known λ_k and σ^2 , all the θ_k and the noises in E are assumed mutually independent.

3 Bayesian regularization: enhanced Gibbs Sampling using overlapping blocks

3.1 Bayesian regularization

Having set the Bayesian model for system identification, our target is now to reconstruct in sampled form the posterior of impulse responses and hyperparameters. This then permits to compute minimum variance estimates of the system coefficients and uncertainty bounds around them. To obtain this, the section is so structured. First, we show that this objective could be obtained resorting to Gibbs sampling, dividing the parameter space in (non overlapping) blocks which are sequentially updated. Since we assume that the number of impulse responses can be considerable, the dimension of the blocks cannot be too large. For instance, due to computational reasons, it would be impossible to update simultaneously all the components of θ . One solution is to resort to a classical Gibbs sampling scheme where any impulse response θ_k is associated with a single block. However, we will see that, in presence of high inputs collinearity, this approach does not work in practice: slow mixing affects the generated Markov chain. The last parts of this section overcome this problem by designing a new stochastic simulation scheme. It exploits additional overlapping blocks to improve the MCMC convergence rate.

3.2 Gibbs sampling

Let $\mathcal{N}(\mu, \Sigma)$ denote the multivariate Gaussian density of mean μ and covariance matrix Σ . From the model assumptions reported in Section 2, one immediately obtains the likelihood of the data and the conditional priors of impulse responses and noises as

$$Y \mid (\{\theta_k\}, \{\lambda_k\}, \sigma^2) \sim \mathcal{N}(G\theta, \sigma^2 I), \quad (5a)$$

$$\theta_k \mid \lambda_k \sim \mathcal{N}(0, \lambda_k K), \quad (5b)$$

$$E \mid \sigma^2 \sim \mathcal{N}(0, \sigma^2 I). \quad (5c)$$

Using Bayes rule, standard calculations lead also to the following *full conditional distributions* of the variables we want to estimate:

$$\lambda_k \mid (Y, \sigma^2, \{\theta_j\}, \{\lambda_j\}_{j \neq k}) \sim \mathcal{I}_g\left(\frac{p+1}{2}, \frac{1}{2} \theta_k' K^{-1} \theta_k\right), \quad (6a)$$

$$\sigma^2 \mid (Y, \{\theta_j\}, \{\lambda_j\}) \sim \mathcal{I}_g\left(\frac{n}{2}, \frac{1}{2} \|Y - G\theta\|^2\right), \quad (6b)$$

$$\theta_k \mid (Y, \sigma^2, \{\lambda_j\}, \{\theta_j\}_{j \neq k}) \sim \mathcal{N}(\hat{\mu}_k, \hat{\Sigma}_k), \quad (6c)$$

where $\mathcal{I}_g(\cdot, \cdot)$ denotes the inverse Gamma distribution and

$$\hat{\mu}_k = \hat{\Sigma}_k \frac{1}{\sigma^2} G_k' (Y - \sum_{j \neq k} G_j \theta_j), \quad (6d)$$

$$\hat{\Sigma}_k = (\lambda_k^{-1}K^{-1} + \frac{1}{\sigma^2}G'_k G_k)^{-1}. \quad (6e)$$

The above equations already allow to implement Gibbs sampling where the following samples are generated at any iteration t :

$$\lambda_k^{(t)} \mid (Y, \sigma^{2(t-1)}, \{\lambda_j^{(t)}\}_{j=1}^{j=k-1}, \{\lambda_j^{(t-1)}\}_{j=k+1}^m, \{\theta_j^{(t-1)}\}), \quad \text{for } k = 1, \dots, m, \quad (7a)$$

$$\sigma^{2(t)} \mid (Y, \{\lambda_j^{(t)}\}, \{\theta_j^{(t-1)}\}), \quad (7b)$$

$$\theta_k^{(t)} \mid (Y, \sigma^{2(t)}, \{\lambda_j^{(t)}\}, \{\theta_j^{(t)}\}_{j=1}^{k-1}, \{\theta_j^{(t-1)}\}_{j=k+1}^m), \quad \text{for } k = 1, \dots, m. \quad (7c)$$

However, as anticipated, such classical approach may have difficulties to handle collinearity. A simple variation consists of a random sweep Gibbs sampling scheme. It updates the blocks $\{\theta_k^{(t)}\}$ randomly, trying to find a strategy to increase the mixing. But it will be shown that this change is not significant enough using numerical examples in Section 5. This motivates the development described in the next sections.

3.3 Overlapping blocks

In our system identification setting, collinearity is related to the relationship between two inputs u_i and u_j which can make some posterior regions difficult to explore. A collinearity measure is now needed to drive the MCMC scheme more towards such parts of the parameter space. In particular, beyond sampling the single θ_i through the full conditional distributions (6c), it is crucial also to update larger blocks. Such blocks should contain e.g. couples of impulse responses with high posterior correlation. Let the inputs u_i be stochastic processes. Then, a first important index is the absolute value of the correlation coefficient, i.e.

$$c_{ij} := \left| \frac{\text{Cov}(u_i, u_j)}{\sqrt{\text{Var}(u_i)\text{Var}(u_j)}} \right|, \quad (8)$$

where $\text{Cov}(\cdot, \cdot)$ and $\text{Var}(\cdot)$ denote the covariance and variance, respectively. If the inputs are not stochastic or their statistics are unknown, such index can be still computed just replacing the variance and covariance in (8) with their estimates, i.e. the sample variance and covariance.

It is now crucial to define a suitable function which maps each c_{ij} into a probability related to the frequency with which the scheme updates the vector containing both θ_i and θ_j at once. First, it is useful to define $\theta_{ij} := [\theta'_i, \theta'_j]'$ and let P_{ij} be the probability connected with the frequency of updating θ_{ij} inside an MCMC iteration. Then,

we use an exponential rule that emphasises correlation coefficients close to one, i.e.

$$P_{ij} = \begin{cases} 0, & i = j; \\ \frac{e^{\beta c_{ij}} - 1}{\text{sum}}, & i \neq j; \end{cases} \quad (9)$$

where $\text{sum} = \sum_{i < j} (e^{\beta c_{ij}} - 1)$ while β is a tuning rate. As an illustrative example, the profile of P_{ij} as a function of c_{ij} with $\beta = 20$ is visible in Fig. 1.

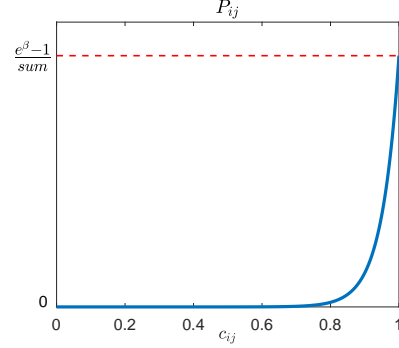


Fig. 1. Probability P_{ij} related to the frequency with which the scheme updates two impulse responses as a function of the index c_{ij} related to their posterior correlation.

Letting $G_{ij} = [G_i, G_j]$, the conditional distribution of θ_{ij} is

$$\theta_{ij} \mid (Y, \sigma^2, \{\theta_k\}_{k \neq i, j}, \{\lambda_k\}) \sim \mathcal{N}(\hat{\mu}_{ij}, \hat{\Sigma}_{ij}) \quad (10a)$$

where

$$\hat{\Sigma}_{ij} = \left(\begin{bmatrix} \lambda_i^{-1}K^{-1} & 0 \\ 0 & \lambda_j^{-1}K^{-1} \end{bmatrix} + \frac{1}{\sigma^2}G'_{ij}G_{ij} \right)^{-1}, \quad (10b)$$

$$\hat{\mu}_{ij} = \hat{\Sigma}_{ij} \frac{1}{\sigma^2} G'_{ij} (Y - \sum_{k \neq i, j} G_k \theta_k). \quad (10c)$$

The above equations may thus complement the Gibbs sampling scheme previously described. They allow to update also additional overlapping blocks consisting of larger pools of impulse responses with a frequency connected to P_{ij} .

3.4 The role of the stable spline kernel scale factors and the use of a common one

The simulation strategy described in the previous section uses a model where the covariance of each impulse response depends on a different stochastic scale factor λ_k . As illustrated via numerical experiments in Section 5, this modeling choice may have a harmful effect in presence of strong collinearity. In fact, it can make the generated chain nearly reducible [12, Chapter 3], i.e. unable to visit the highly correlated parts of the posterior.

The problem can be overcome by reducing the model complexity, i.e. assigning a common scale factor to all the impulse responses covariances. This can appear a paradox since one could think that a model with more parameters may permit the chain to move more easily along the posterior's support. Instead, the introduction of many scale factors can trap the algorithm in regions from which it is virtually impossible to escape. Using only one common scale factor for all the θ_k covariances, the distribution (6a) becomes

$$\lambda | (Y, \sigma^2, \{\theta_k\}) \sim \mathcal{I}_g\left(\frac{np+1}{2}, \frac{1}{2} \sum \theta'_k K^{-1} \theta_k\right) \quad (11)$$

and the update of λ , previously defined by (7a), is given by

$$\lambda^{(t)} | (Y, \sigma^{2(t-1)}, \{\theta_k^{(t-1)}\}). \quad (12)$$

In turn, at step t of the MCMC algorithm, in place of differently from (7c), the algorithm will sample θ_k using

$$\theta_k^{(t)} | (Y, \sigma^{2(t)}, \lambda^{(t)}, \{\theta_j^{(t)}\}_{j=1}^{k-1}, \{\theta_j^{(t-1)}\}_{j=k+1}^m). \quad (13)$$

Finally, when the block θ_{ij} is selected, the update rule becomes

$$\theta_{ij}^{(t)} | (Y, \sigma^{2(t)}, \lambda^{(t)}, \{\theta_k^{(t)}\}_{k \neq i, j}), \quad (14)$$

i.e. (10) is now used with $\lambda_i = \lambda_j = \lambda^{(t)}$.

3.5 Random sweep sampling schemes: the RSGSOB algorithm

By working upon all the developments previously described, in this section we finalize our MCMC strategy for linear system identification under collinear inputs. Besides updating the scale factor and noise variance using (12) and (7b), we have also to define the exact rule to update the blocks and overlapping blocks during any iteration. For this purpose, we will extend the so called random sweep Gibbs sampling scheme including overlapping blocks. The main idea is that at any iteration only one of the blocks $\{\theta_i, \theta_{ij}\}$ is updated, chosen according to a discrete probability density function of the scalars P_{ij} introduced in Section 3.3. The symmetries $c_{ij} = c_{ji}$, $P_{ij} = P_{ji}$, and the fact that θ_{ij} and θ_{ji} contain the same impulse responses coefficients, imply that only the blocks θ_{ij} with $i < j$ need to be considered in what follows.

Let $\mathcal{M}_1 := \{\theta_i\}$ and $\mathcal{M}_2 := \{\theta_{ij}\}_{i < j}$ and define

$$\mathcal{M} := \mathcal{M}_1 \cup \mathcal{M}_2.$$

Now, we specify for any block in \mathcal{M} the probability of being selected by the random sweep sampling scheme. It is natural to assign the same probability to the blocks in \mathcal{M}_1 . For what concerns the overlapping ones, we need

Algorithm 1 Random sweep Gibbs samplings with overlapping blocks using one common scale factor (**RS-GSOB**)

Input: Measurements G, Y ; initial values $\lambda^{(0)}, \sigma^{2(0)}, \{\theta_k^{(0)}\}; \alpha, \beta, n_{OB}, n_B$.

Output: Estimate $\hat{\theta}$.

- 1: Calculate $\{P_{ij}\}$ from input data for $i \leq j$ in (9);
 - 2: **for** $t = 1 : n_{MC}$ **do**
 - 3: Sample (12), (7b) in sequence;
 - 4: **for** $s = 1 : m + n_{OB}$ **do**
 - 5: Choose a block b from the distribution $\{P_{\mathcal{M}}\}$;
 - 6: **if** $b = \theta_i \in \mathcal{M}_1$ **then**
 - 7: Sample (6c) given the latest data of θ and update the values of $\theta_i^{(t)}$;
 - 8: **else** $\{b = \theta_{ij} \in \mathcal{M}_2\}$
 - 9: Sample (14) given the latest data of $\theta^{(t)}$ and update the values of $\theta_i^{(t)}$ and $\theta_j^{(t)}$.
 - 10: **end if**
 - 11: **end for**
 - 12: **end for**
 - 13: Calculate $\hat{\theta}$ as the mean of the impulse responses samples from $t = n_B + 1$ to $t = n_{MC}$.
-

to take into account the collinearity indexes discussed in Section 3.3. Overall, the discrete probability density $P_{\mathcal{M}}$ over \mathcal{M} is then defined by

$$P_{\mathcal{M}}(b) = \begin{cases} \frac{1}{m+n_{OB}}, & \text{if } b = \theta_i \in \mathcal{M}_1, \\ \frac{n_{OB}}{m+n_{OB}} P_{ij}, & \text{if } b = \theta_{ij} \in \mathcal{M}_2, \end{cases} \quad (15)$$

so that $\sum_{\mathcal{M}} P_{\mathcal{M}}(b) = 1$ for any $n_{OB} \in \mathbb{Z}_+$ which represents a tuning parameter. It regulates how frequently we want to consider the collinearity problem during our sampling.

Finally, our random sweep Gibbs samplings with overlapping blocks is summarized in Algorithm 1 where n_{MC} indicates the number of MCMC steps while n_B is the length of the burn-in [12, Chapter 7]. The procedure is called RSGSOB in what follows.

4 Convergence analysis

4.1 The main convergence theorem

In this section we show that RSGSOB generates a Markov chain convergent to the desired posterior of impulse responses and hyperparameters. In addition, the speed of convergence is characterized. Finally, a simple example is reported to illustrate the practical implications of our theoretical findings.

We consider the convergence rate in the L^2 sense in the

setting of spectral analysis, as initially proposed by [14]. This includes the study of how quickly the expectations of arbitrary square h -integrable functions approach their stationary values. Since θ is the parameter really of interest to estimate, we focus on the convergence rate of the main part in Algorithm 1, i.e., from line 4 to line 11. It is then natural to introduce the following definition.

Definition 1 (Convergence rate) Let $h^{(t)}(\theta \mid \theta^{(0)})$ denote the probability density of a Markov chain at time t given the starting point $\theta^{(0)}$. Assume that the Markov chain converges to the probability density function h and denote by $\mathbb{E}_{h(\theta)}[f(\theta)]$ the expectation of a real-valued function f under h with respect to θ , i.e.,

$$\mathbb{E}_{h(\theta)}[f(\theta)] = \int f(\theta)h(\theta)d\theta.$$

Let

$$P^t(f) := \int f(\theta)h^{(t)}(\theta \mid \theta^{(0)})d\theta$$

describe the expectation of $f(\theta)$ with respect to the density of the Markov chain at time t given $\theta^{(0)}$. Then, the convergence rate of θ given $\theta^{(0)}$ is the minimum scalar rate such that for all the square h -integrable functions f , and for all $r > \text{rate}$, one has

$$\lim_{t \rightarrow \infty} \mathbb{E}_{h(\theta^{(0)})} [\{P^t(f) - \mathbb{E}_{h(\theta)}[f(\theta)]\}^2] r^{-t} = 0. \quad (16)$$

Hence, rate quantifies how fast the density of the Markov chain approaches the true distribution in L^2 as t grows to infinity.

Note that, according to the above definition, the convergence rate is independent of the initial chain value. Additional details on the nature of this notion of convergence can be found in [38], where the rates are derived for different Gibbs sampling schemes involving Gaussian distributions.

Our convergence result, whose proof can be found in Appendix, is reported below. To formulate it, we use $\rho(\cdot)$ to denote the spectral radius, i.e., the maximum eigenvalue modulus of a matrix, while the relevant probability distributions contained in its statement are calculated in Appendix.

Theorem 2 (Convergence of RSGSOB) The RSGSOB scheme described in Algorithm 1 generates a Markov chain convergent to the correct posterior of impulse responses and hyperparameters in accordance with the Bayesian model for linear system identification described in Section 2. In addition, for fixed hyperparameters λ and σ^2 , the convergence rate in Definition 1 is

$$\text{rate}(\text{RSGSOB}) = \rho(C^{m+n_{OB}}) = \rho(C)^{m+n_{OB}}, \quad (17)$$

where

$$\begin{aligned} C &:= \sum_{\mathcal{M}_1} P_{\mathcal{M}}(\theta_i)C_i + \sum_{\mathcal{M}_2} P_{\mathcal{M}}(\theta_{ij})C_{ij} \\ &= \frac{1}{m+n_{OB}} \left(\sum_{\mathcal{M}_1} C_i + n_{OB} \sum_{\mathcal{M}_2} P_{ij}C_{ij} \right), \end{aligned} \quad (18)$$

the matrices C_i and C_{ij} are reported, respectively, in (A.3c) and (A.2c) with $\lambda^{(t)} = \lambda$ and $\sigma^{2(t)} = \sigma^2$.

4.2 A simple example

While more sophisticated system identification problems are discussed in the next section, a simple example is now introduced to show that the use of overlapping blocks, the key feature of RSGSOB, can fasten the convergence in comparison with a classical random sweep Gibbs sampling (RSGS) scheme. This latter procedure, also described in the next section in TABLE 1, samples the blocks θ_i with the same probability $1/m$ for $m+n_{OB}$ times during any iteration. Its convergence rate is obtained below using Lemma 7 and Lemma 8 contained in Appendix.

Proposition 3 (Convergence rate of RSGS) With hyperparameters λ and σ^2 fixed, the convergence rate of RSGS is

$$\text{rate}(\text{RSGS}) = \rho\left(\frac{1}{m} \sum_{i=1}^m C_i\right)^{m+n_{OB}}, \quad (19)$$

where the matrix C_i is defined in (A.3c).

Now, consider a toy and extreme example where all the correlation coefficients among the inputs are equal to one. In particular, we set $\lambda = 1$ while the noise variance is $\sigma^2 = 1$ and consider a system with 10 inputs, all equal to a Dirac delta function. It comes that the regression matrix G in (2) has dimension 10×100 and any G_i is the identity matrix. Setting $n_{OB} = 3$, $\alpha = 0.9$, and $\beta = 100$, from (17) and (19) one obtains

$$\begin{aligned} \text{rate}(\text{RSGSOB}) &= 0.5861, \\ \text{rate}(\text{RSGS}) &= 0.8045. \end{aligned}$$

This outlines how the use of RSGSOB can greatly enhance the convergence rate of the MCMC procedure.

5 Simulation examples

5.1 Example 1: an extreme case

We first illustrate one extreme case of collinearity where the system is fed with two identical inputs. This simple

example will point out the importance of introducing overlapping blocks in the sampling scheme and of adopting only a common scale factor λ for all the impulse responses.

Let $u_1(t) = u_2(t)$, with the common input defined by realizations of white Gaussian noise with $n = 500$. Let also $F_1(z), F_2(z)$ be two randomly generated transfer functions with a common denominator of degree 5, displayed in the panels of Fig. 2. The measurement noises e_i are independent Gaussians of variance equal to the sample variance of $\sum_{k=1}^2 F_k u_k$ divided by 5. In the Fisherian framework adopted by classical system identification impulse responses estimation is a non-identifiable problem. But we can use the model (2) with the dimension of θ_1 and θ_2 set to $p = 50$ within the Bayesian framework. The goal is to find the impulse responses posterior under the stable spline prior (3) where here, and in Example 2, the variance decay rate is $\alpha = 0.9$.

In this example, one has the number of inputs $m = 2$ and the collinearity index $c_{12} = 1$, so that $P_{12} = 1$. We also set $n_{OB} = 2$ in (15) obtaining $P_{\mathcal{M}}(\theta_1) = P_{\mathcal{M}}(\theta_2) = 1/4$, and $P_{\mathcal{M}}(\theta_{12}) = 1/2$. We run $n_{MC} = 500$ Monte-Carlo iterations in MATLAB to compare 6 algorithms described in Table 1, where our proposed Algorithm 1 is abbreviated to RSGSOB, and highlighted bold, while RSGSOBd is the version which adopts different scale factors, one for any stable spline kernel modeling θ_k . The other algorithms include Gibbs sampling with one or multiple scale factors, respectively called GS and GSd, Random sweep Gibbs sampling with one or multiple scale factors, respectively called RSGS and RSGSd.

The posterior of the two impulse responses is reconstructed using samples from MCMC considering the first 50% as burn-in. Results coming from the six procedures are displayed in Fig. 2, where true impulse responses are the red thick lines. For clarity, the scale of the vertical axis of Fig. 2(e) is different from other sub-figures in Fig. 2.

Let us start commenting the performance of the algorithms using only one common scale factor. Results show that only RSGSOB returns an informative posterior, able to highlight the non-identifiability issues, see Figs. 2(e). Results from classical Gibbs sampling (GS) and Random sweep Gibbs sampling (RSGS) are in Figs. 2(a) and 2(c). These two algorithms have similar performance, not significantly affected by choosing deterministic or random sampling scheme (this also holds in Example 2, so that we will hereby only use RSGS in Table 1 as a benchmark). As a matter of fact, both of them have not reached the level of information on the posterior shape returned by RSGSOB since they converge much slower to the target density. The use of GS or RSGS, e.g. for control or prediction purposes, can thus lead to erroneous results, possibly affected by huge errors if future inputs are not very similar. In

addition, differently from RSGSOB, they can largely underestimate the uncertainty around the predictions.

For what regards the algorithms that use multiple scale factors, their performance is really poor. Figs. 2(b) and 2(f) show that the samples of the second impulse response θ_2 are close to zero. The reason is that chains with multiple scale factors may easily become nearly reducible. In fact, during the first MCMC iterations, the algorithm generates an impulse response θ_1 able to explain the data. Hence, θ_2 is virtually set to zero, so that also λ_2 becomes very small. This scale factor becomes a strong (and wrong) prior for θ_2 during all the subsequent iterations. This in practice forces the sampler to always use only θ_1 to describe the experimental evidence. A minor phenomenon to mention is that one can see from Figs. 2(c) and 2(d) that random sweep Gibbs sampling, which does not use overlapping blocks, decreases the negative influence of using different scale factors, but remains affected by slow mixing.

5.2 Example 2: identification of large-scale systems

Now, we use 100 inputs to test the algorithms in large-scale systems identification. This is a situation where it is crucial to divide the parameter space into many small blocks for computational reasons. Otherwise, at any MCMC iteration one should multiply and invert large matrices whose dimension depends on the overall number of impulse response coefficients.

The collinear inputs are generated as follows

$$u_j(t) = u_i(t) + r_{ij}(t), \quad (20)$$

where $r_{ij}(t)$ is a noise independent of $u_i(t)$. To increase collinearity between inputs and also the level of ill-conditioning affecting the problem, $r_{ij}(t)$ in (20) is a moving average (MA) process,

$$r_{ij}(t) = v_{ij}(t) - 0.8v_{ij}(t-1),$$

where $v_{ij}(t) \sim \mathcal{N}(0, \omega_{ij}^2)$. From (8), one has

$$c_{ij} = \frac{|\eta_i|}{\sqrt{\eta_i^2 + \omega_{ij}^2/(1-0.8^2)}},$$

when $u_i(t)$ is a zero mean process with variance η_i^2 . Hence, one can see that the amount of collinearity can be tuned by ω_{ij} .

The data set size is $n = 10^5$. We introduce correlation among the first 10 inputs by letting

$$u_{i+1}(t) = u_i(t) + r_{(i+1)i}(t), \quad (21)$$

Table 1
6 algorithms to compare in Example 1

Abbr.	Algorithm	Update in one iteration
GS	Gibbs sampling	(12)(7b)(13) in sequence
GSd	GS using different scale factors	(7a)(7b)(7c) in sequence
RSGS	Random sweep Gibbs sampling	first (12)(7b), then repeat $m + n_{OB}$ times: randomly choose and update a block in $\{\theta_i\}$ with the same probability $1/m$
RSGSd	RSGS using different scale factors	the same as RSGS, except for updating (7a) instead of (12)
RSGSOB	RSGS with overlapping blocks (Algorithm 1)	line 3 to line 11 in Algorithm 1
RSGSOBd	RSGSOB using different scale factors	the same as RSGSOB, except for updating (7a) instead of (12)

for $i = 1, \dots, 9$, where the first input $u_1(t)$ is white and Gaussian of variance 1, $r_{(i+1)i}(t)$ is obtained by setting the $c_{i(i+1)} = 0.99$ for $i = 1, 2, \dots, 9$. The other 90 inputs, i.e. $\{u_i\}_{i=11}^{100}$ are zero-mean standard i.i.d. Gaussian processes of variance 1.

The different collinearity levels of the first 10 inputs are summarized by the correlation coefficient matrix (calculated from the input realizations) reported in Fig. 3. One can see that the input pairs have correlation coefficients ranging from about 0.99 to about 0.91.

We set $\beta = 100$ and use (9) to define the probabilities of selecting the overlapping blocks at any iteration. The P_{ij} related to the first 10 impulse responses are shown in Fig. (4) (a) with a sharing colorbar. The P_{ij} for $i, j > 10$ are obviously all close to zero: the associated impulse responses couples do not have significant correlation. Instead, inside all the pairs $(i, j)(i \neq j)$ considered for constructing overlapping blocks, the couples $(i, i + 1)$ ($i = 1, \dots, 9$) of highest collinearity are assigned near 7% of the total amount of probability. The couple (1, 10), which has a correlation coefficient 0.9135, is given 0.0063%.

We generate random transfer functions $F_i(z)$ ($i = 1, \dots, 100$) of degree 5 with a common denominator. The Gaussian noises e_i have variance $\sigma^2 = 7.243$ which corresponds to 0.3 times the variance of the process $\sum_{k=1}^{100} F_k u_k$. Model (2) is adopted with each impulse response of order $p = 50$ and only results coming from RSGSOB and RSGS are shown, letting $\alpha = 0.9$, $n_{OB} = 10$ and $n_{MC} = 1000$. The pie charts in Fig. (4) (b) display the frequencies with which the blocks have been selected after running RSGSOB. The one in the right panel regards all the blocks $\{b; b \in \mathcal{M}\}$. One can see that the frequency of sampling blocks in \mathcal{M}_2 is close to $\sum P_{\mathcal{M}}(b \in \mathcal{M}_2) = 1/11$. The middle panel displays

Table 2
Hyperparameters and convergence rates in Example 2

Algorithm \ Variables	$\hat{\lambda}$	$\hat{\sigma}^2$	rate
RSGS	0.6785	7.730	0.9930
RSGSOB	0.6790	7.722	0.8919

the frequencies concerning only the blocks $\{b; b \in \mathcal{M}_2\}$, i.e., this is a pie chart specific for the 8.9% marked data in the right panel. The same colorbar adopted in Fig. (4) (a) is used, with the index pairs as labels for different θ_{ij} . As expected, the pair (i, j) is sampled more frequently according to the growth of the correlation indicated by the P_{ij} values. During the simulation none of the blocks $\theta_{ij} \in \mathcal{M}_2$ with $i, j > 10$ is sampled due to very small associated P_{ij} values.

To better appreciate the difference between the results coming from RSGSOB and RSGS, first it is useful to compute their convergence rates. This is obtained using, respectively, Theorem 2 and Proposition 3, with hyperparameters set to their estimates $\hat{\lambda}$ and $\hat{\sigma}^2$ computed from the first 200 MCMC samples. Results are shown in TABLE 2: the convergence rates are 0.89 for RSGSOB and 0.99 for RSGS, suggesting that the proposed algorithm will converge much faster. To quantify this aspect we adopt the Raftery-Lewis criterion (RLC) described in [12, Chapter 7]. Such algorithm is given a pilot analysis consisting of the first samples generated by an MCMC scheme. Then, it determines in advance the number of initial samples M that need to be discarded to account for the burn-in and the number of samples N necessary to estimate percentiles of the posterior of any parameter with a certain accuracy. We generate 10 pilot analyses, each consisting of the first 200 samples generated by RSGSOB and RSGS. Then, we use RLC to obtain the maximum values of M and

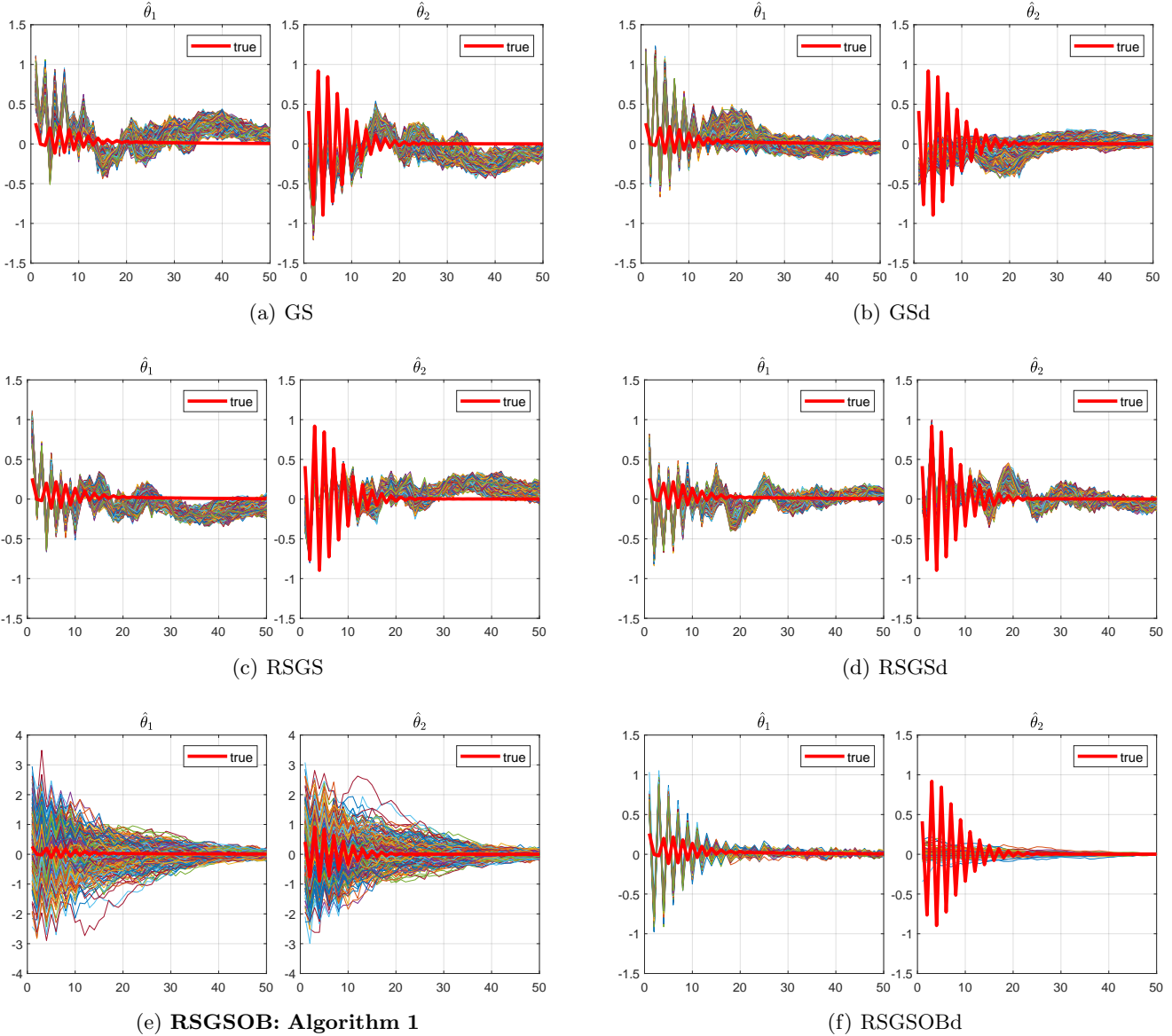


Fig. 2. *Example 1*: posterior of the two impulse responses reconstructed in sampled form after 500 iterations by the 6 algorithms described in Table 1.

N to estimate the percentile 2.5% of the coefficients of the first 10 impulse responses with accuracy 0.02 and probability 0.95. Results are displayed in Fig. 5. The average of the burn-in length M for RSGSOB and RSGS is, respectively, around 33 and 1340. The average of the required samples N is instead, respectively, around 2000 and 10500. These results well point out the computational advantages of RSGSOB: the use of overlapping blocks much decreases the number of iterations needed to converge to the target posterior and to visit efficiently its support. In particular, in view of the small burn-in, samples from the desired posterior can be obtained after few MCMC steps.

Now, the MCMC estimates obtained by RSGSOB and RSGS are illustrated. First, we focus on the first 10 impulse responses related to the strongly collinear inputs. Fig. 6 shows the true impulse responses (red) together with the posterior mean (blue) and the 95% uncertainty bounds (dashed) computed by the first 100 samples. While RSGSOB already returns good estimates and credible confidence intervals, the outcomes from RSGS are not reliable. The same results after 200 iterations are displayed in Fig. 7. RSGS results improve but are still quite far from those returned by RSGSOB.

The quality of the estimators is finally measured by com-

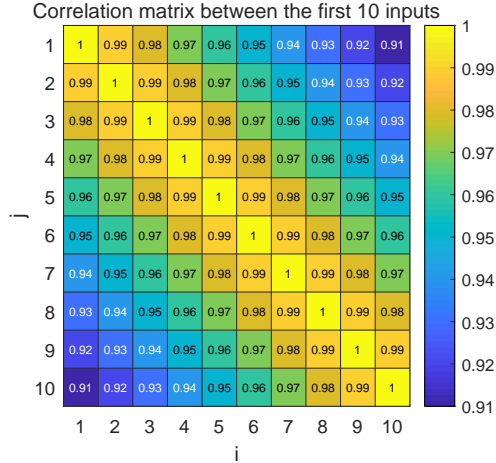


Fig. 3. *Example 2*: collinearity indexes $\{c_{ij}\}$ of the input couples $\{(u_i, u_j)\}_{i,j=1}^{10}$.

putting the fit measures: given an unknown vector x and its estimate \hat{x} , it is given by

$$fit(\hat{x}) := 100 \left(1 - \frac{\|x - \hat{x}\|}{\|x\|} \right),$$

with $\|\cdot\|$ to indicate the Euclidean norm. Specifically, the fits for algorithms RSGS and RSGSOB are compared in TABLE 3, for different number of MCMC samples used to compute the posterior mean and setting x to three different vectors θ , θ_{col} and θ_{ind} . The first vector θ contains all the 100 impulse responses while the second gathers only the first 10 impulse responses (hard to estimate due to collinearity), i.e.

$$\theta_{col} = [\theta'_1, \dots, \theta'_{10}]'.$$

Finally, the third vector contains the remaining 90 impulse responses (easier to estimate)

$$\theta_{ind} = [\theta'_{11}, \dots, \theta'_{100}]'.$$

As expected, the performance is similar when θ_{ind} has to be estimated while the best possible fits for θ_{col} are reached by RSGSOB after few iterations, confirming the predictions of the RLC.

6 Conclusion

Identification of large-scale linear dynamic systems may be complicated by two important factors. First, the number of unknown variables to be estimated may be large. So, when the problem is faced in a Bayesian framework using MCMC to reconstruct the posterior of the impulse response coefficients in θ , any step of the algorithm can be computationally expensive. In fact, chain generation

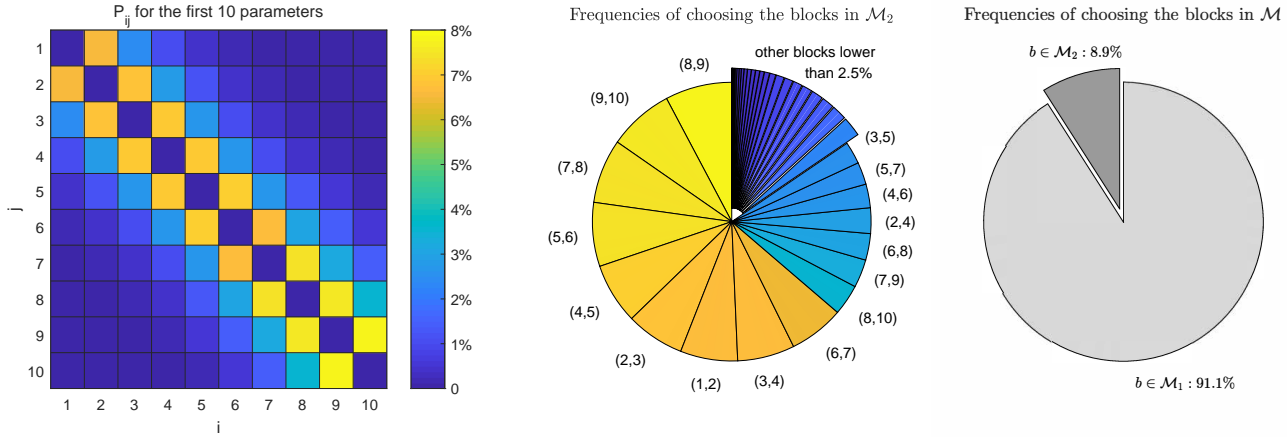
Table 3
sum of fits in Example 2

100 iterations		$fit(\hat{\theta})$	$fit(\hat{\theta}_{col})$	$fit(\hat{\theta}_{ind})$
Algorithm				
	RSGS	-15.2	-231.2	71.6
	RSGSOB	65.7	29.5	73.9
200 iterations		$fit(\hat{\theta})$	$fit(\hat{\theta}_{col})$	$fit(\hat{\theta}_{ind})$
Algorithm				
	RSGS	61.2	10.9	74.0
	RSGSOB	65.5	28.5	73.9
1000 iterations		$fit(\hat{\theta})$	$fit(\hat{\theta}_{col})$	$fit(\hat{\theta}_{ind})$
Algorithm				
	RSGS	65.1	25.2	74.5
	RSGSOB	66.4	30.2	74.6
2000 iterations		$fit(\hat{\theta})$	$fit(\hat{\theta}_{col})$	$fit(\hat{\theta}_{ind})$
Algorithm				
	RSGS	65.8	27.7	74.7
	RSGSOB	66.6	30.9	74.7

requires to invert a matrix of very large dimension to draw samples from the full conditional distributions of θ . Hence, it is important to design strategies where small groups of variables are updated. Second, ill-conditioning can affect the problem due to input collinearity. This problem can be e.g. encountered in the estimation of dynamic networks where feedback and algebraic loops are often present. It leads to slow mixing of the generated Markov chains. This aspect requires a careful selection of the blocks of variables to be sequentially updated. An MCMC strategy for identification of large-scale dynamic systems based on the stable spline prior has been here proposed to address both of these issues. It relies on Gibbs sampling complemented with a strategy which also updates some relevant overlapping blocks. The updating frequencies of such blocks are regulated by the level of collinearity among different system inputs. The proposed algorithm has been analyzed under a theoretical perspective, proving its convergence and deriving also the convergence rate, also showing its effectiveness through simulated studies.

References

- [1] H. Akaike. A new look at the statistical model identification. *IEEE Trans. on Automatic Control*, AC-19:716–723, 1974.
- [2] A. Aravkin, J.V. Burke, A. Chiuso, and G. Pillonetto. On the estimation of hyperparameters for empirical bayes estimators: Maximum marginal likelihood vs minimum mse. *IFAC Proceedings Volumes*, 45(16):125 – 130, 2012.
- [3] A.S. Bazanella, M. Gevers, J.M. Hendrickx, and A. Parraga. Identifiability of dynamical networks: Which nodes need be measured? In *2017 IEEE 56th Annual Conference on Decision and Control (CDC)*, pages 5870–5875, 2017.



(a) Probability level P_{ij} associated to the frequency of choosing overlapping blocks for $\{\theta_i\}_{i=1}^{10}$ when adopting RSGSOB. (b) Pie charts of the chosen blocks. **Left:** frequencies with which the overlapping blocks $b \in \mathcal{M}_2$ have been selected by RSGSOB. **Right:** frequencies with which all the blocks $b \in \mathcal{M}$ have been selected by RSGSOB.

Fig. 4. Statistical indexes useful to evaluate how RSGSOB have sampled the different impulse responses blocks to deal with collinearity in Example 2.

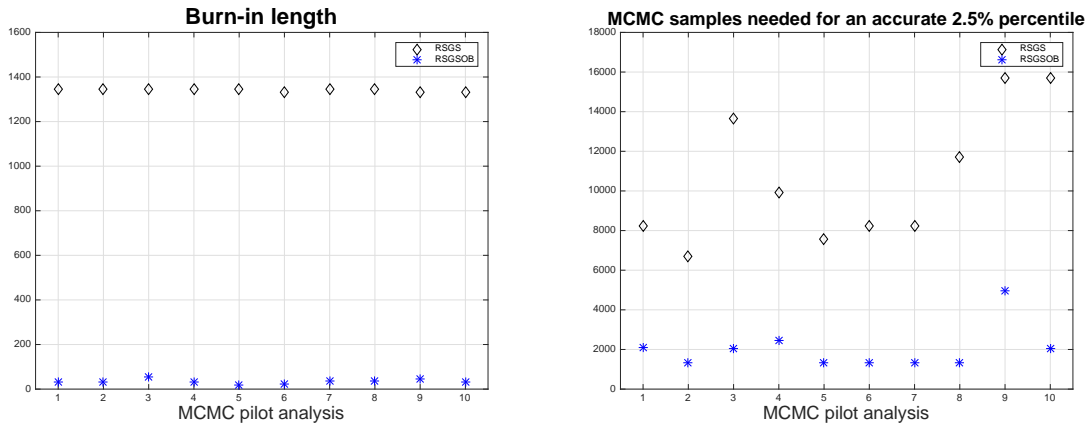


Fig. 5. Raftery-Lewis applied to 10 pilot analyses generated by RSGSOB and RSGS: maximum values of the burn-in length (left) and of the number of samples needed to estimate the percentile 2.5% of the coefficients of the first 10 impulse responses with accuracy 0.02 and probability 0.95.

[4] B.M. Bell and G. Pillonetto. Estimating parameters and stochastic functions of one variable using nonlinear measurement models. *Inverse Problems*, 20(3):627, 2004.

[5] D. A. Belsley and R. E. Welsch. *Regression Diagnostics: Identifying Influential Data and Sources of Collinearity*. Wiley, New York, 1980.

[6] G. Bottegal, H. Hjalmarsson, and G. Pillonetto. A new kernel-based approach to system identification with quantized output data. *Automatica*, 85:145–152, 2017.

[7] W. Cao, A. Lidnquist, and G. Picci. Modeling of low rank time series.

[8] W. Cao, G. Picci, and A. Lidnquist. Identification of low rank vector processes. *Automatica*, 2023.

[9] A. Chiuso and G. Picci. On the ill-conditioning of subspace identification with inputs. *Automatica*, 40(4):575–589, 2004.

[10] A. Chiuso and G. Pillonetto. A Bayesian approach to sparse dynamic network identification. *Automatica*, 48(8):1553–1565, 2012.

[11] S.J.M. Fonken, M. Ferizbegovic, and H. Hjalmarsson. Consistent identification of dynamic networks subject to white noise using weighted null-space fitting. In *Proc. 21st IFAC World Congress, Berlin, Germany*, 2020.

[12] W.R. Gilks, S. Richardson, and D.J. Spiegelhalter. *Markov chain Monte Carlo in Practice*. London: Chapman and Hall, 1996.

[13] J. Goncalves and S. Warnick. Necessary and sufficient conditions for dynamical structure reconstruction of LTI networks. *IEEE Transactions on Automatic Control*, 53(7):1670–1674, 2008.

[14] J. Goodman and A. Sokal. Multigrid Monte Carlo Method. Conceptual foundations. *Physical Review D*, 40(6):2035–2071, 1989.

[15] P. Hagmann, L. Cammoun, X. Gigandet, R. Meuli, C.J. Honey, V.J. Wedeen, and O. Sporns. Mapping the structural core of human cerebral cortex. *PLOS Biology*, 6(7):1–15, 2008.

[16] T. J. Hastie, R. J. Tibshirani, and J. Friedman. *The*

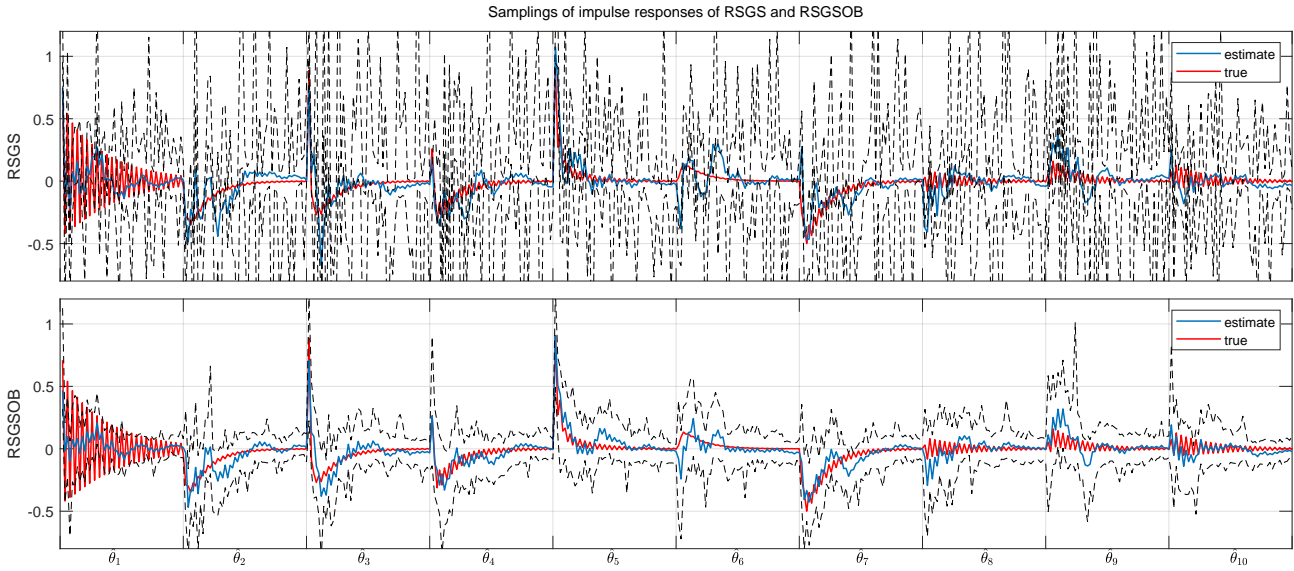


Fig. 6. True impulse responses (red) together with the mean (blue) and the 95% uncertainty bounds (dashed) computed by the first 100 samples of $\{\theta\}_{i=1}^{10}$.

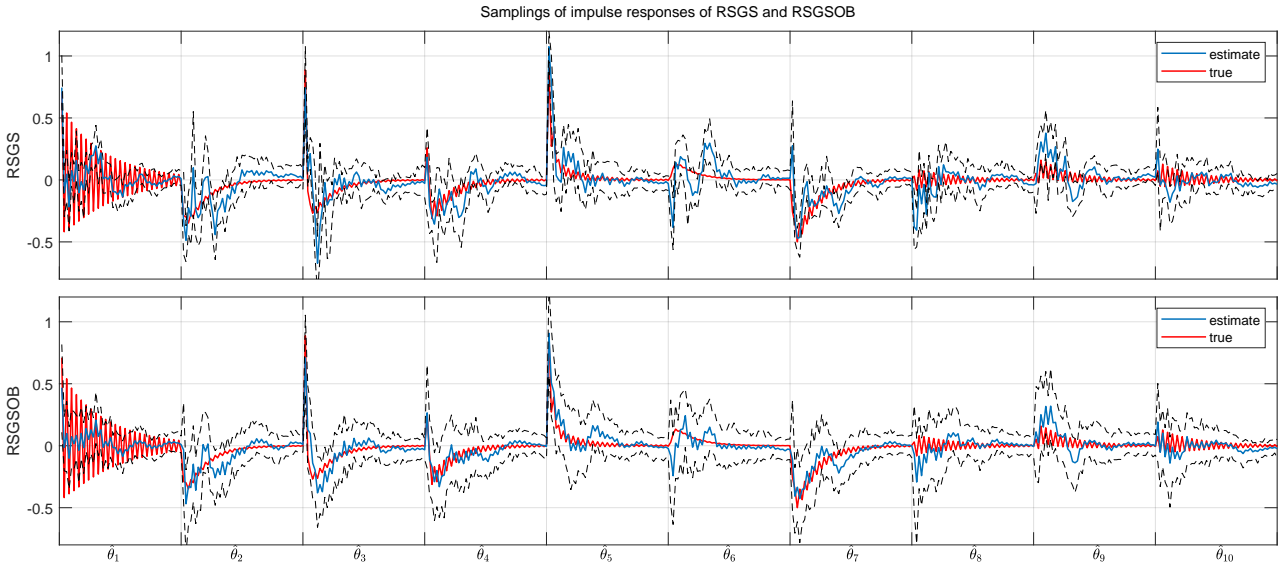


Fig. 7. True impulse responses (red) together with the mean (blue) and the 95% uncertainty bounds (dashed) computed by the first 200 samples of $\{\theta\}_{i=1}^{10}$.

Elements of Statistical Learning. Data Mining, Inference and Prediction. Springer, Canada, 2001.

- [17] J.M. Hendrickx, M. Gevers, and A.S. Bazanella. Identifiability of dynamical networks with partial node measurements. *IEEE Transactions on Automatic Control*, 64(6):2240–2253, 2019.
- [18] R. Hickman, M.C. Van Verk, A.J.H. Van Dijken, M.P. Mendes, I. A. Vroegop-Vos, L. Caarls, M. Steenberg, I. Van der Nagel, G.J. Wesselink, A. Jironkin, A. Talbot, J. Rhodes, M. De Vries, R.C. Schuurink, K. Denby, C.M.J. Pieterse, and S.C.M. Van Wees. Architecture and dynamics of the jasmonic acid gene regulatory network. *The Plant Cell*, 29(9):2086–2105, 2017.
- [19] H. Jeffreys. An invariant form for the prior probability in estimation problems. *Proc. R. Soc. Lond.*, 186:453–461, 1946.
- [20] S. Liverani, A. Lavigne, and M. Blangiardo. Modelling collinear and spatially correlated data. *Spatial and Spatio-temporal Epidemiology*, 18:63–73, 2016.
- [21] L. Ljung. *System Identification - Theory for the User.* Prentice-Hall, Upper Saddle River, N.J., 2nd edition, 1999.
- [22] D. Materassi and G. Innocenti. Topological identification in networks of dynamical systems. *IEEE Transactions on Automatic Control*, 55(8):1860–1871, 2010.
- [23] J. Molitor, M. Papatomas, Mi. Jerrett, and S. Richardson. Bayesian profile regression with an application to the national survey of children’s health. *Biostatistics*, 11(3):484–498, July 2010.
- [24] G.A. Pagani and M. Aiello. The power grid as a complex network: A survey. *Physica A: Statistical Mechanics and its Applications*, 392(11):2688–2700, 2013.
- [25] G. Pillonetto, A. Aravkin, D. Gedon, L. Ljung, A. H. Ribeiro, and T.B. Schön. Deep networks for system identification: a survey, 2023.
- [26] G. Pillonetto, T. Chen, A. Chiuso, G. De Nicolao, and L. Ljung. *Regularized System Identification.* Springer, 2022.
- [27] G. Pillonetto and A. Chiuso. Tuning complexity in regularized kernel-based regression and linear system identification: The robustness of the marginal likelihood estimator. *Automatica*, 58:106 – 117, 2015.
- [28] G. Pillonetto, A. Chiuso, and G. De Nicolao. Regularized estimation of sums of exponentials in spaces generated by stable spline kernels. In *Proceedings of the IEEE American Conf. Conf., Baltimore, USA*, 2010.
- [29] G. Pillonetto, A. Chiuso, and G. De Nicolao. Prediction error identification of linear systems: a nonparametric Gaussian regression approach. *Automatica*, 47(2):291–305, 2011.
- [30] G. Pillonetto and G. De Nicolao. A new kernel-based approach for linear system identification. *Automatica*, 46(1):81–93, 2010.
- [31] G. Pillonetto, F. Dinuzzo, T. Chen, G. De Nicolao, and L. Ljung. Kernel methods in system identification, machine learning and function estimation: a survey. *Automatica*, 50(3):657–682, 2014.
- [32] G. Pillonetto and A. Scampicchio. Sample complexity and minimax properties of exponentially stable regularized estimators. *IEEE Trans. Automat. Contr.*, 2021.
- [33] A. Pitard and J. F. Viel. Some methods to address collinearity among pollutants in epidemiological time series. *Statistics in Medicine*, 16(5):527–544, 1997.
- [34] G. Prando, M. Zorzi, A. Bertoldo, M. Corbetta, M. Zorzi, and A. Chiuso. Sparse DCM for whole-brain effective connectivity from resting-state fmri data. *NeuroImage*, 208:116367, 2020.
- [35] K.R. Ramaswamy and P.M. J. Van den Hof. A local direct method for module identification in dynamic networks with correlated noise. *IEEE Transactions on Automatic Control*, 2021.
- [36] C.E. Rasmussen and C.K.I. Williams. *Gaussian Processes for Machine Learning.* The MIT Press, 2006.
- [37] G. O. Roberts. Simple conditions for the convergence of the gibbs sampler and metropolis-hastings algorithms. *Stochastic Processes and their Applications*, 49:207–216, 1994.
- [38] G. O. Roberts and S. K. Sahu. Updating schemes, correlation structure, blocking and parameterization for the Gibbs sampler. *Journal of the Royal Statistical Society*, 59(2):291–317, 1997.
- [39] T. Söderström and P. Stoica. *System Identification.* Prentice-Hall, 1989.
- [40] C. Srisa-An. Guideline of collinearity - avoidable regression models on time-series analysis. In *2021 2nd International Conference on Big Data Analytics and Practices (IBDAP)*, pages 28–32, 2021.
- [41] P.M.J. Van den Hof, A.G. Dankers, P.S.C. Heuberger, and X. Bombois. Identification of dynamic models in complex networks with prediction error methods: basic methods for consistent module estimates. *Automatica*, 49(10):2994–3006, 2013.
- [42] H.H.M. Weerts, P.M. J. Van den Hof, and A.G. Dankers. Prediction error identification of linear dynamic networks with rank-reduced noise. *Automatica*, 98:256–268, 2018.
- [43] Z. Yue, J. Thunberg, W. Pan, L. Ljung, and J. Goncalves. Dynamic network reconstruction from heterogeneous datasets. *Automatica*, 123:109339, 2021.
- [44] J. Zhang, Z. Wang, X. Zheng, L. Guan, and C. Y. Chung. Locally weighted ridge regression for power system online sensitivity identification considering data collinearity. *IEEE Transactions on Power Systems*, 33(2):1624–1634, March 2018.
- [45] Hongpeng Zhou, Chahine Ibrahim, Wei Xing Zheng, and Wei Pan. Sparse bayesian deep learning for dynamic system identification. *Automatica*, 144:110489, 2022.

A Proof of Theorem 2

A.1 Preliminary lemmas

We start reporting five lemmas which are instrumental for the proof of RSGSOB convergence. The first three derive from direct calculations which exploit the algorithmic structure of RSGSOB. In particular, the first one gives useful distributions in Section 4.

Lemma 4 ($p(\theta^s | Y, \sigma^{2(t)}, \lambda^{(t)}, \theta^{s-1}, b)$) *At the t -th iteration of Algorithm 1, given a chosen block b , the conditional distribution of θ from sub-iteration step $s - 1$ to s is Gaussian, i.e.,*

$$\theta^s | Y, \sigma^{2(t)}, \lambda^{(t)}, \theta^{s-1}, b \sim \mathcal{N}(\hat{\mu}^s, \hat{\Sigma}^s). \quad (\text{A.1})$$

Two cases now arises:

When $b = \theta_{ij}$,

$$\hat{\mu}^s = C_{ij}\theta^{s-1} + c_{ij}, \quad (\text{A.2a})$$

The fourth lemma is an important convergence result obtained in [38], while the last one regards the spectral radius of a matrix power whose proof is reported for the sake of completeness.

Lemma 7 (Theorem 3, [38]) *Consider the following random scan sampler. Let C_i , $1 \leq i \leq n$, be $m \times m$ matrices and Ψ_i , $1 \leq i \leq n$, be $m \times m$ non-negative definite matrices. Given $\theta^{(t)}$, $\theta^{(t+1)}$ is chosen from*

$$N(C_i \theta^{(t)} + c_i, \Psi_i),$$

with probability p_i , $0 \leq p_i \leq 1$ for each i and $\sum p_i = 1$. Thus at each transition the chain chooses from a mixture of autoregressive alternatives. For this chain, the convergence rate is the maximum modulus eigenvalue of the matrix

$$C = \sum_{i=1}^n p_i C_i.$$

Lemma 8 *The spectral radius of a matrix power is the power of the matrix's spectral radius, i.e.,*

$$\rho(A^m) = \rho(A)^m.$$

PROOF. Any matrix A can be written as $A = PJP^{-1}$, with J the Jordan canonical form of A , then $C^m = PJ^mP^{-1}$. And hence the eigenvalues of A^m are the m power of all eigenvalues of A . Denote by $\varphi(A)$ the characteristic polynomial of A . Since for any complex number $\zeta \in \mathbb{C}$, $|\zeta^m| = |\zeta|^m$, we have

$$\begin{aligned} \rho(A^m) &= \max\{|\zeta|; \varphi_{A^m}(\zeta) = 0\} \\ &= \max\{|\zeta^m|; \varphi_A(\zeta) = 0\} \\ &= \max\{|\zeta|^m; \varphi_A(\zeta) = 0\} = \rho(A)^m. \end{aligned}$$

□

A.2 Proof of Theorem 2

To prove the first part of the theorem regarding the convergence of RSGSOB, the first step is to show that the Markov chain generated by this algorithm has invariant density $p(\cdot)$ given by the target posterior. This is a consequence of the Metropolis-Hastings algorithm. The update of σ^2 and λ done inside each step of RSGSOB is standard since it exploits their full conditional distributions. Hence, the invariance of p is guaranteed. Now, let us focus on the update of θ and use $p(\cdot|\cdot)$ to indicate the transition density that selects randomly a block and updates it. Such transition density can be written as $p(\cdot|\cdot) = \sum_b P_b p_b(\cdot|\cdot)$ where $\sum_b P_b = 1$ and each $p_b(\cdot|\cdot)$ can update either just one of the impulse responses θ_k (type one) or the couple θ_k, θ_j denoted by $\theta_{k,j}$ (type two) through full-conditional distributions. Without loss of

generality, we change the values of these proposal densities over a set of null probability measure. Specifically, for type one we set $p_b(\theta^*|\theta^\#) = 0$ if the block θ_k contained in θ^* contains the same values of the block θ_k in $\theta^\#$. For type two, we set $p_b(\theta^*|\theta^\#)$ if the vector θ_k in θ^* coincides with the vector θ_k in $\theta^\#$ or if the vector θ_j in θ^* coincides with the vector θ_j in $\theta^\#$.

Assume that two vectors θ^s and θ^{s-1} are compatible with the evolution of RSGSOB after one sub-iteration, i.e. they may differ only in the values contained e.g. in the b -th block. The acceptance rate is

$$\begin{aligned} &\min \left\{ 1, \frac{p(\theta^s) \sum_b P_b p_b(\theta^{s-1} | \theta^s)}{p(\theta^{s-1}) \sum_b P_b p_b(\theta^s | \theta^{s-1})} \right\} \\ &= \min \left\{ 1, \frac{p(\theta^s) p_{b^*}(\theta^{s-1} | \theta^s)}{p(\theta^{s-1}) p_{b^*}(\theta^s | \theta^{s-1})} \right\}, \end{aligned}$$

where the last equality comes from the fact that $p_b(\theta^s|\theta^{s-1}) = p_b(\theta^{s-1}|\theta^s) = 0$ for any $b \neq b^*$. Then, by Bayes rules,

$$\begin{aligned} &\frac{p(\theta^s)}{p(\theta^{s-1}) p_{b^*}(\theta^s | \theta^{s-1})} p_{b^*}(\theta^{s-1} | \theta^s) \\ &= \frac{p(\theta^s)}{p(\theta^{s-1}) p_{b^*}(\theta^s | \theta^{s-1})} \frac{p_{b^*}(\theta^s | \theta^{s-1}) p(\theta^{s-1})}{p(\theta^s)} \quad (\text{A.8}) \\ &= 1. \end{aligned}$$

Since this holds for any block b^* , the acceptance rate is always equal to one. This means that, if the selected block is accepted with probability 1, the Metropolis-Hastings rule is followed. This is exactly what is done by RSGSOB and this implies that such algorithm generates a Markov chain with invariant density $p(\cdot)$. Now, to complete the first part of the proof of the theorem, we need to prove that the Markov chain converges to the invariant density. For an MCMC algorithm, this holds if the chain is irreducible and aperiodic [12]. These properties are satisfied by RSGSOB. In fact, in (A.6) the conditional distributions of $\sigma^{2(t)}$ and $\lambda^{(t)}$ are inverse gamma from (12), (7b), hence are continuous and greater than 0 in the regions $D_{\sigma^2} = \mathbb{R}_+$, $D_\lambda = \mathbb{R}_+$. Since $\pi^{(t)}(\theta^s | \theta^{s-1})$ in (A.4) is a weighted sum of Gaussian distributions from (A.4)(A.1)-(A.3), it is continuous and greater than zero in the region $D_\theta = \mathbb{R}^{mp}$, so as the nested integration $p(\theta^{(t)} | Y, \sigma^{2(t)}, \lambda^{(t)}, \theta^{(t-1)})$ from (A.7). As a result, the transition probability (A.6) is continuous in $D := D_\theta \times D_{\sigma^2} \times D_\lambda$, inducing irreducibility directly.

Now, letting $\gamma := (\theta, \sigma^2, \lambda)$, we prove that the chain is aperiodic. For some initial $\gamma^{(0)}$, define the region

$$B^{(t)} = \{\gamma^{(t)} \in D; p(\gamma^{(t)} | \gamma^{(0)}, Y) > 0\}. \quad (\text{A.9})$$

For any specific value $\gamma^* \in B^{(t)}$, $t \geq 1$, we have $K(\gamma^* | \gamma^*) > 0$. Hence there exists an open neighbourhood of

γ^* , $B^{(t)*} \subseteq B^{(t)}$, and $\varepsilon(\gamma^*) > 0$ such that, for all $\gamma^\# \in B^{(t)*}$,

$$K(\gamma^* | \gamma^\#) \geq \varepsilon(\gamma^*) > 0,$$

i.e., lower semi-continuous at 0 (see [37]). It follows that the transition probability from the initial time to the instant t satisfies

$$\begin{aligned} p(\gamma^{(t+1)} = \gamma^* | \gamma^{(0)}, Y) &= \int K(\gamma^* | \gamma^\#) p(\gamma^{(t)} = \gamma^\# | \gamma^{(0)}, Y) d\gamma^\# \\ &\geq \varepsilon(\gamma^*) \int_{B^{(t)*}} p(\gamma^{(t)} = \gamma^\# | \gamma^{(0)}, Y) d\gamma^\# > 0. \end{aligned}$$

Thus, from the definition in (A.9), $\gamma^* \in B^{(t+1)}$ as well, ensuring aperiodicity and hence convergence.

Finally, to prove the last part of the theorem, the convergence rate is derived as follows. From Lemma 4, given θ^s , θ^{s+1} is sampled from (A.1) with probability (15). Then since this process is repeated for $m + n_{OB}$ times, and by Lemma 7, we have

$$rate = \rho(C^{m+n_{OB}}).$$

Then by Lemma 8, (17) holds.